Multimodal Plasmonic Biosensing Nanostructures Prepared by DNA-Directed immobilization of Multifunctional DNA-Gold Nanoparticles

Nuria Tort[1,2,‡], J.-Pablo Salvador[2,1] and M.-Pilar Marco[1.2]*

[1]*Nanobiotechnology for Diagnostics (Nb4D), IQAC-CSIC.* [2] *CIBER de Bioingeniería, Biomateriales y Nanomedicina (CIBER-BBN). Jordi Girona 18-26, 08034-Barcelona, Spain*

*To whom correspondence should be sent:

M.-Pilar Marco

IQAC-CSIC

Jordi Girona, 18-26

08034-Barcelona, Spain

Phone: 93 4006180

FAX: 93 2045904

E-mail: pilar.marco@cid.csic.es

‡, Present Address of Nuria Tort:

Biokit, S.A.

Can Malé

08186 Lliçà d'Amunt

Spain

Con formato: Color de fuente: Automático

Con formato: Color de fuente: Automático

ABSTRACT

Biofunctional multimodal plasmonic nanostructures suitable for multiplexed localized surface plasmon resonance (LSPR) biosensing have been created by DNA-directed immobilization (DDI) of two distinct multifunctional biohybrid gold nanoparticles. Gold nanoparticles (AuNP) of distinct sizes, and therefore showing distinct plasmon resonant peaks (RP), have been biofunctionalized and codified with two different single stranded-DNA (ssDNA) chains. One of these oligonucleotide chains has been specifically designed to direct each AuNP to a distinct location of the surface of a DNA microarray chip through specific hybridization with complementary oligonucleotide strands. Scanning Electron Microscopy (SEM) has been used to demonstrate selective immobilization of each AuNP on distinct spots. The second ssDNA chain of the AuNPs provides the possibility to introduce by hybridization distinct types of bioactive molecules or bioreceptors, on a reversible manner. In this work, hapten-oligonucleotide bioconjugate probes, with sequences complementary to the second ssDNA linked to the AuNP, have been synthesized and used to create multiplexed hapten-biofuncionalized plasmonic nanostructures. The oligonucleotide probes consist on anabolic androgenic steroid haptens (AAS) covalently linked to specifically designed oligonucleotide sequences. The biofunctionality of these plasmonic nanostructures has been demonstrated by fluorescent microarray immunoassay and LSPR measurements, recording the shift of the RP produced after the antibody binding to the corresponding hapten-oligonucleotide probes immobilized on the nanostructured surface. Preliminary data show that this approach could allow manufacturing multifunctional multimodal LSPR chips for multiplexed analysis of different substances reaching very good detectability. Thus, small molecular weigh, analytes such as stanozolol (ST,) could be detected at concentrations in the low nM range. The results here presented open the door for an easy way to construct site-encoded multiplexed multimodal LSPR sensor transducers, combining the DDI strategies with multimodal biohybrid nanoparticles showing distinct optical properties.

KEYWORDS: DNA-gold nanoparticles, hapten-oligonucleotide bioconjugates, DNA-directed Immobilization (DDI), Localized Surface Plasmon Resonance (LSPR), multifunctional plasmonic nanostructures, multiplexed biosensor, Anabolic-Androgenic Steroids (AAS).

Con formato: Color de fuente: Automático

1. INTRODUCTION

Nanoparticle-based optical biosensors, like those based on the localized surface plasmon resonance (LSPR) principle, have proven to be suitable for the quantitative detection of chemical and biological targets (Estevez et al. 2014; Hill 2015; Li et al. 2015; Li et al. 2009; Sriram et al. 2015; Willets and Van Duyne 2007;Kreuzer, 2008 #22; Zhao et al. 2006). LSPR is an optical phenomenon generated when an incident photon or electromagnetic field such as light interacts with a metal nanoparticle producing the collective oscillation of the conductive electrons at their surface at a particular frequency known as resonant peak (RP) (Bohren 1983). When these nanostructures interact with a light beam, part of the incident photons are absorbed and part are scattered in different directions. Consequently, optical spectroscopy is the simplest method to detect the LSPR on metal nanostructures (Willets and Van Duyne 2007). The LSPR spectral position is highly dependent on the composition, size or shape of the nanoparticles, as well as the refractive index of the dielectric medium and the spacing between them (Liz-Marzán 2005; Sonnichsen et al. 2005; Yamamichi et al. 2009). Typical materials for plasmonic applications are noble metals, especially silver and gold; despite silver displays more intense LSPR bands than gold, the higher chemical stability of gold nanostructures has favored its preferential application for biosensing (Estevez et al. 2014; Hill 2015; Li et al. 2015; Lv et al. 2015; Wang and Ma 2009).

LSPR multiplexed platforms can be accomplished through non-planar (in solution) and planar (nanostructured surfaces) arrays. Non-planar multiplexed arrays (see reviews (Anker et al. 2008; Hu et al. 2006; Mannelli and Marco 2010; Mayer and Hafner ; Petryayeva and Krull 2011)), in which the biomolecular interaction with the targets takes place in solution, can be prepared by combining nanoparticles of different sizes (30-120 nm)(Yu and Irudayaraj 2007), shapes (nanospheres, nanorods, nanocages, nanostars, etc.), materials (single metal, nanoshells or alloys) or through self-assembly of plasmonic nanoparticles which allows expanding the library of plasmonic nanostructures with tunable, coupled optical properties (Klinkova et al. 2014). However for immunosensing applications separation of the biocomplexes formed on top of the nanoparticle surface is usually required. Moreover, the multiplexing capability of these systems is often limited by the number of nanoparticles showing distinct RPs and their bandwidths which often lead to overlapped signals. Planar arrays, as solid-phase immunoassays, can facilitate separation of the biocomplexes and removal of interfering sample matrix components providing at the same time increased multiplexed capabilities based on site codification of the bioreceptors. Thus, a LSPR planar microarray chip combining nanoparticles of different RPs

Código de campo cambiado
Código de campo cambiado
Código de campo cambiado
Código de campo cambiado
Código de campo cambiado
Código de campo cambiado
Código de campo cambiado

would allow dual identification of the targets based on the location and also on the nanoparticles optical properties.

Nanostructured planar arrays can be fabricated using advanced lithographic techniques like electron beam lithography (EBL) or focused ion beam (FIB). These techniques permit an accurate control of the size, shape and spatial distribution of the nanoparticles, allowing manufacturing a wide variety of two dimensional (2D) or quasi-three-dimensional (Q3D) metal nanostructures (nanoholes, nanopillars, nanocrescents, etc.) with particular enhanced plasmonic properties suitable for biosensing (Bhushan and Matsui 2010; Graells 2007; Guillot and de la Chapelle 2012; Li et al. 2015; Lv et al. 2015; Zhou et al. 2016). However, these techniques are expensive and the patterned regions are small, which difficult the development of applications raising at the same time the cost of potential commercial sensing devices based on those nanostructures. Alternatively, LSPR planar arrays can also be constructed by immobilizing colloidal nanoparticles onto solid supports through different chemistries. Different synthetic approaches have been reported to obtain a wide variety of nanoparticle shapes (nanospheres, nanorods, nanostars, nanoprisms, etc.) made of different noble metals and with tunable sizes(Sriram et al. 2015). Once synthesized they can be immobilized through i) electrostatic interactions, using proteins or polyelectrolytes adsorbed on the nanoparticles surface (Li et al. 2009), ii) high affinity interactions, like the existing between biotin and streptavidin (Grabar et al. 1995; Reinhard et al. 2005) or iii) exploiting the high affinity of gold and silver colloids towards amino or mercapto functional groups, present on glass surfaces upon silanization (Fujiwara et al. 2006; Grabar et al. 1995; Kreuzer et al. 2008; Kreuzer et al. 2006; Yamamichi et al. 2009). However, these approaches lack of the necessary flexibility to create LSPR sensing surfaces in which different nanoparticles have to be immobilized selectively on different sites.

DNA-directed immobilization (DDI), based on the self-organizing capabilities and the highly specificity of the DNA hybridization, allows immobilizing potentially any type of biomolecule onto a DNA-biofunctionalized surface (see (Meyer et al. 2014; Seymour et al. 2015; Tan et al. 2014) for recent review papers), including small organic molecules. Thus, we have reported the possibility of manufacturing multiplexed hapten-microarrays by hybridizing hapten-oligonucleotide probes with complementary ssDNA strands immobilized on distinct spots of a DNA microarray (Tort et al. 2012a; Tort et al. 2009). DDI has also been used to immobilize nanoparticles using DNA biofunctionalized nanoprobes (Loweth et al. 1999; Peschel et al. 2002; Reichert et al. 2000; Wolfgang and Taton 2003). However, to our knowledge no examples exist on the use of DDI to create nanostructured surfaces with plasmonic properties for biosensing applications. With this scenario, we report here for the first time the development of a

Código de campo cambiado
Código de campo cambiado
Código de campo cambiado
Código de campo cambiado
Código de campo cambiado
Código de campo cambiado
Código de campo cambiado

multiplexed (multiple target analytes) and multimodal (multiple RPs) LSPR biosensor using biofunctional plasmonic nanostructured chips manufactured on a DNA microarray using DDI to address distinct multifunctional AuNPs to predefined positions of a surface. As a proof of concept, we have used these chips to detect Anabolic Androgenic Steroids (AAS) for which immunoreagents are available in our laboratory (Salvador et al. 2007; Salvador et al. 2008, 2009; Tort et al. 2012b; Tort et al. 2009).

2. MATERIALS AND METHODS

2.1. Reagents and Immunoreagents.

The preparation and characterization of the immunoreagents for Stanozolol (ST, As147), Tetrahydrogestrinone (THG, As170), Boldenone (B, As138) and Fluoroquinolones (FQ, As172) used in this study have been described before (Calvo et al. 2009; Pinacho et al. 2012; Salvador et al. 2007; Salvador et al. 2008, 2009; Tort et al. 2012b). ST was purchased from Sequoia Research Products, Ltd. (Oxford, UK). THG was synthesized in our laboratory (Salvador et al. 2007). Stock solutions of analytes were prepared at 10mM concentration in DMSO. The oligonucleotides with amine and thiol moieties at the 5' end (*N1down/up*, *N2down/up*, *N3down/up*, *N4down/up*) were ordered to Sigma-Aldrich®. The synthesis of the hapten-oligonucleotide conjugates (ST: 8-$N_{1}up$; THG: hG-$N_{2}up$, B: 13-$N_{3}up$ and FQ: FQ-$N_{4}up$) has already been described(Tort et al. 2012a). The sequences of these oligonucleotides are shown in table S1 of the Supporting Information document. The anti-rabbit IgG-TRITC (antibody against rabbit IgGs labelled with tetramethylrhodamine) was purchased from Sigma-Aldrich®. Other chemical reagents were purchased from Aldrich Chemical Co. (Milwaukee, WI). The O-(methyl)-O'-(2-mercaptoethyl)-hexaethylene glycol (m-PEG-SH) was supplied by Polypure. Chloroauric acid ($HAuCl_4{\cdot}3H_2O$), trisodium citrate ($Na_3C_6H_5O_7{\cdot}2H_2O$) and N-hydroxylamine from Sigma-Aldrich® were employed for the synthesis of gold nanoparticles (AuNPs). Glycerol and Tris Base were employed for the final suspension of the synthesized AuNP-DNA conjugates. NaN_3 was used as preservative of the final conjugates. DL-dithiothreitol (DTT) was purchased from Sigma-Aldrich®.

2.2. Buffers

PBS was 0.01 M phosphate buffer in a 0.8% saline solution (137 mmol L^{-1} NaCl, 2.7 mmol L^{-1} KCl), and the pH was 7.5. PBST was PBS with 0.05% Tween 20. Printing buffer consisted of 150mM sodium phosphate (pH 8.5) with 0.01% sodium dodecyl sulphate (SDS). Hybridization buffer was 10 mM TRIS, 1mM EDTA, 1M NaCl (pH 7.2). The final washing buffer was saline-sodium citrate buffer (SSC) (15 mM NaCl + 1.5 mM sodium citrate, 0.05% SDS; pH 7.5). Disulfide cleavage buffer was 170 mM phosphate buffer (pH 8.0). Final reconstitution buffer of the AuNP-DNA conjugates

was 20% glycerol, 20 mM Tris base, 0.05% NaN_3. For LSPR measurements the slides were washed with 0.3M ammonium acetate, pH 7.0.

2.3. Materials and Instruments.

NAP-5 columns (Sephadex G-25) were purchased from Pharmacia Biotech. COSTAR® 96 well UV Microplates, with UV transparent flat bottom and the plain microscope slides used to prepare the microarrays were from CORNING (Tewksbury, USA). pH and conductivity values of all buffers and solutions were measured with a 540 GLP pH meter and a LF 340, conductimeter (WTW, Weilheim, Germany), respectively. The immobilization of the capture amine-oligonucleotides on the glass slides in spots (100 µm) was performed with a BioOdissey Calligrapher MiniArrayer (Bio-Rad Laboratories, inc. USA). Fluorescent measurements were recorded on a ScanArray® Gx PLUS (Perkin Elmer, USA) using a green laser with an optical emission filter at 543 nm with 5 µm resolution. The laser power and PMT were set to 90% and 70%, respectively. The spots were measured by F543_Mean-B543 (Mean Cy3 foreground intensity minus mean Cy3 background intensity). Fluorescence intensity values are expressed in relative fluorescence units (RFUs) as average and standard deviation of at least 10 replicate spots in three replicate wells. The characterization of the AuNPs was performed using a PHILIPS CM30 transmission electron microscope (TEM) and a UV-vis spectrophotometer. The nanostructured surfaces were characterized using an ultra-high resolution electron microscopy (NovaNano SEM 230, FEI Company) of the Nanotechnology platform at the Parc Cientific de Barcelona. The optical setup consisted of an inverted microscope (Nikon, Ti-U). The extinction spectra of the gold colloids were measured by conventional dark-field spectroscopy (Dry DF Condenser, NA=0.90-0.80). The sample illumination was performed with a halogen lamp (100 W). The light scattered by the particles was collected by an objective lens (×10 with NA = 0.3 and working distance of 1.6 mm), fiber-coupled to a multimode fiber (fiber diameter = 400 µm) and sent toward a CCD-cooled spectrometer (Shamrock SR-303i, Andor). The competitive curves were analyzed with a four parameter logistic equation using the software SoftmaxPro v4.7 (Molecular Devices) and GraphPad Prism v 6 (GraphPad Software Inc., San Diego, CA) according to the following formula: $Y = [(A - B)/1 - (x/C)^D] + B$, where A is the maximal fluorescence, B is the minimum fluorescence, C is the concentration producing 50% of the difference between A and B (or IC_{50}), and D is the slope at the inflection point of the sigmoid curve. The limit of detection (LOD) is defined as the concentration producing 90% of the maximum fluorescence (IC_{90}).

2.4. Synthesis of Gold Nanoparticles (AuNPs)

AuNP20 were synthesized by the citrate method following the procedure reported by Turkevich (Enustun 1963; Turkevich 1951) and Frens (Frens 1973). The AuNPs were characterized in

Con formato: Fuente: +Cuerpo (Calibri), 11 pto, Negrita, Inglés (Estados Unidos)

Con formato: Párrafo de lista, Sangría: Izquierda: 0 cm, Primera línea: 0 cm, Esquema numerado + Nivel: 2 + Estilo de numeración: 1, 2, 3, … + Iniciar en: 1 + Alineación: Izquierda + Alineación: 0,63 cm + Sangría: 1,4 cm

Con formato: Fuente: +Cuerpo (Calibri), Inglés (Estados Unidos)

Con formato: Color de fuente: Automático

Con formato: Color de fuente: Automático

Con formato: Color de fuente: Automático

Con formato: Fuente: +Cuerpo (Calibri), 11 pto, Negrita, Inglés (Estados Unidos)

Con formato: Párrafo de lista, Sangría: Izquierda: -0,01 cm, Sangría francesa: 0,01 cm, Esquema numerado + Nivel: 2 + Estilo de numeración: 1, 2, 3, … + Iniciar en: 1 + Alineación: Izquierda + Alineación: 0,63 cm + Sangría: 1,4 cm

Con formato: Fuente: +Cuerpo (Calibri), Negrita, Inglés (Estados Unidos)

Código de campo cambiado

Código de campo cambiado

solution, by UV-Vis spectrometry and by TEM, taking several pictures of each batch of particles. The size of these nanoparticles was assessed measuring the diameters of a significant number of nanoparticles (n=50) supplied by TEM images. A mean size of 18.8 ± 2.4 nm (13% dispersion) was obtained with a concentration of 7·1011 AuNP mL^{-1}, estimated considering the initial amount of Au (50 µg mL^{-1}) and assuming a quantitative reduction (Au3+ à Au0) (see figure 1S in the Supporting Information (SI) document)

AuNP40 were synthesized following the N-hydroxylamine reduction method developed by Brown (Brown et al. 1999) and also employed by Haiss (Haiss et al. 2007), using the AuNP20 as seeds. In this procedure, additional Au3+ is reduced at room temperature on the surface of the seeds increasing their diameter. A mean size of 40.3 ± 3.3 nm (n=50, 8 % dispersion) was obtained according to TEM analysis at a concentration of $7 \cdot 10^{10}$ AuNP mL^{-1} (see figure S1 in the SI document)

2.5. Synthesis of the AuNP20-*N_3up/N_1down* and AuNP40-*N_4up/N_2down* Biohybrid Multifunctional Nanoparticles

The oligonucleotide sequences coupled to the gold nanoparticles of 20 nm (AuNP20) and 40 nm (AuNP40) are listed in Table S1. The coupling of the oligonucleotides to the AuNPs was carried out following the procedures described by Taton (Taton 2001) and Hill (Hill and Mirkin 2006). First of all, the potential oligonucleotide oxidized fraction, with 5'-disulfide functionality, was reduced by adding a solution of 0.1 M DTT (DL-dithiothreitol in disulfide cleavage buffer, 100 µL) to the lyophilized oligonucleotide sample (5 nmols), kept at RT for 2-3 h and purified with a NAP-5 column. A UV-visible spectrophotometer at 260 nm was used for monitoring the elution of the DNA and to determine the concentration using the Beer's Law (A=ε.c.l). Then, thiol-terminated oligonucleotides (1.25 nmols of a 1:1 mixture of *N_1downSH* and *N_3upSH* for the AuNP20 and 0.5 nmols of a 1:1 mixture of *N_2downSH* and *N_4upSH* for the AuNP40), were added to the corresponding gold colloidal solutions (5 mL, AuNP20: $7 \cdot 10^{11}$ nanoparticles mL^{-1} and AuNP40: $7 \cdot 10^{10}$ nanoparticles mL^{-1}). The mixtures were then incubated overnight (12 h) at RT protected to the light. Multiple small additions of 1M NaCl and 0.1M phosphate buffer (PB) were performed to reach 0.1 M NaCl and 10 mM phosphate buffer concentrations, and then, the biohybrid nanoparticles were incubated for 12 h more at RT. Afterwards, the mixtures were centrifuged, and the biohybrid AuNPs (red oil) were resuspended in 1 mM m-PEG-SH (5 mL) solution for 1 h. Finally, the biohybrid AuNPs were centrifuged two times in water, and after the third centrifugation, they were resuspended in the final reconstitution buffer (1 mL) 5 times concentrated. The biohybrid nanoparticles were stored at 4ºC protected to the light until use.

2.6. Preparation of Multifunctional Multimodal Plasmonic Nanostructured Surfaces

Código de campo cambiado
Código de campo cambiado
Con formato: Fuente: +Cuerpo (Calibri), 11 pto, Negrita, Inglés (Estados Unidos)
Con formato: Párrafo de lista, Sangría: Izquierda: 0 cm, Primera línea: 0 cm, Esquema numerado + Nivel: 2 + Estilo de numeración: 1, 2, 3, … + Iniciar en: 1 + Alineación: Izquierda + Alineación: 0,63 cm + Sangría: 1,4 cm
Con formato: Fuente: +Cuerpo (Calibri), 11 pto, Inglés (Estados Unidos)
Con formato: Fuente: +Cuerpo (Calibri), 11 pto, Negrita, Inglés (Estados Unidos)
Con formato: Fuente: +Cuerpo (Calibri), Negrita, Inglés (Estados Unidos)
Código de campo cambiado
Código de campo cambiado
Con formato: Fuente: +Cuerpo (Calibri), 11 pto, Negrita, Inglés (Estados Unidos)
Con formato: Párrafo de lista, Sangría: Izquierda: 0 cm, Primera línea: 0 cm, Esquema numerado + Nivel: 2 + Estilo de numeración: 1, 2, 3, … + Iniciar en: 1 + Alineación: Izquierda + Alineación: 0,63 cm + Sangría: 1,4 cm
Con formato: Fuente: +Cuerpo (Calibri), Negrita, Inglés (Estados Unidos)

1. DNA microarray: Epoxysilane activated slides were prepared in the laboratory by deeping the slides on a 10% (w/v) NaOH solution for 1h at RT, followed by a derivatization with a 2.5% (v/v) 3-glycidoxypropyltrimethoxysilane (GPTMS) solution in anhydrous ethanol for 3h at RT. Then, the capture oligonucleotide chains (*N_3-downNH$_2$ and N_4-downNH$_2$* at 200 µg/mL in printing buffer) were spotted onto the epoxy-activated slides in a controlled humidity chamber at 60% and maintained for 3h at RT. The DNA funcrionalized slides could be stored until use for about 1 month at 4 ºC on a dry chamber. ***2. Immobilization of the multifunctional DNA AuNP.*** The printed slides were placed on a microplate microarray ArrayIt® hardware system allowing 96-well formatted experimentation with up to four glass substrate slides (Telechem International Inc.). The system is provided of a silicon gasket that demarcates 24 wells for slide. On each well, there was a microarray with a defined number of spots, depending of the experiment. Before starting, the slides were washed four times with PBST and afterwards, the biohybrid AuNP-DNA (AuNP20-*N_3up/N_1down*, AuNP40-*N_4up/N_2down* or both) were added onto the microarray (100 µL/well) at different concentrations (from 10^{10} to 10^{12} nanoparticles/mL, depending on the conjugate and on the assay), incubated for 30 min at RT, washed and dried. Under these conditions the slides could be stored at 4 ºC on a dry chamber for more than 1 month, although in most of the experiments, the slides were immediately used or the day after for the assays.

2.7. Fluorescent Microarray Immunoassay

General Protocol. A solution of the corresponding hapten-oligonucleotide bioconjugate (8-*N_1up*, hG-*N_2up*, 13-*N_3up* or FQ-*N_4up,* 1 µg/mL in hybridization buffer), or an equimolar mixture of them, was added (100 µL/well) to the corresponding microarray wells of a glass slide where the multifunctional biohybrid AuNPs had been immobilized. For certain control experiments the slides had been functionalized with just the *NxdownNH$_2$* oligonucleotides. The mixture was incubated for 30 min at RT and rinsed with PBST. Then, a solution of the corresponding specific antiserum (As147, As170, As138 or As172 diluted 1/1000 in PBST), or a mixture of them, was added (100 µL/ well) to the corresponding microarray wells and incubated for 30 min at RT. Following, the slide was washed again with PBST and finally, an anti-IgG-TRITC solution (1/250 in PBST) was added (100 µL/well). After an incubation of 30 min at RT, the slide was washed with the final washing buffer, dried with N_2 and read with the scanner.

Competitive Assay. Solutions of the standards (0.064-1000 nM ST or/and THG in PBST) were added to the microarray wells (50 µL/well in PBST), treated with the hapten-oligonucleotide conjugates and washed as described before, followed by the corresponding antiserum (As147 diluted 1/2000 and As170 diluted 1/1000 in PBST 50 µL/well) and processed as described above (see figure 3S on the SI).

Con formato: No ajustar espacio entre texto latino y asiático, No ajustar espacio entre texto asiático y números

Con formato: Fuente: +Cuerpo (Calibri)

Con formato: Fuente: +Cuerpo (Calibri), 11 pto, Negrita, Inglés (Estados Unidos)

Con formato: Párrafo de lista, Sangría: Izquierda: 0 cm, Primera línea: 0 cm, Esquema numerado + Nivel: 2 + Estilo de numeración: 1, 2, 3, … + Iniciar en: 1 + Alineación: Izquierda + Alineación: 0,63 cm + Sangría: 1,4 cm

Con formato: Fuente: +Cuerpo (Calibri), Negrita, Inglés (Estados Unidos)

2.8. LSPR measurements

The slides prepared and processed as described above, except for the antiIgG-TRITC, were washed the 0.3 M ammonium acetate buffer, dried with N_2 and read with the dark-field microscope connected to a spectrometer to record the LSPR spectra and to measure the RP shift.

3. RESULTS AND DISCUSSION

3.1. Design and preparation of multifunctional biohybrid AuNP for AAS

With the aim to demonstrate the feasibility of DDI for manufacturing multiplexed multimodal LSPR immunosensors for biosensing applications, we addressed the preparation multimodal plasmonic nanostructures using thoroughly designed multifunctional biohybrid nanoparticles. Based on the specificity and self-organized capabilities of DNA, the design took into consideration *i)* the necessity to direct the particles selectively onto defined spots of a DNA microarray surface, and *ii)* the need to interact with analytical targets. Hence, we proposed the preparation of nanoparticles biofunctionalized with two different ssDNA strands. Oligonucleotide sequences generically named N_x*upSH* and N_y*downSH* (where, *Nx* or *Ny,* means a particular oligonucleotide sequence, and the term *up* or *down*, is used to describe the relative position on the hybridization event, see Figure 1~~Figure 1~~) were designed and synthesized with the necessary SH functionality to bind the AuNP. N_x*upSH* had to be complementary to the oligonucleotide strands (N_x*downNH*$_2$*)* previously immobilized on the spots of the glass surface (DNA microarray), and N_y*downSH* had to be complementary to biomolecule-N_y*up* bioconjugates addressed to specifically recognize the analytical targets.

As proof-of concept, we focused on AAS, a particular family of steroids used illegally as doping agents in sportive competitions to improve athletic performance, and as growth-promoters in farms to increase meat production. Immunochemical determination of AAS takes place under competitive configurations due to their small molecular size (see figure 3S in SI). Previously, we already demonstrated the possibility to simultaneously quantify AAS on a multiplexed ELISA (Tort et al. 2012b) and on a hapten microarray created on a glass surface by DDI using hapten-oligonucleotide probes as competitors (Tort et al. 2009). In this work, we have followed the same approach, but immobilizing those hapten-oligonucleotide probes (hapten-N_y*up* bioconjugates) on the AuNPs surface through the hybridization with their complementary ssDNA chains to obtain a multifunctional hapten biofunctionalized nanostructured surface. Stanozolol (ST) and tetrahydrogestrinone (THG) were selected as model target analytes and the corresponding hapten-oligonucleotide probes, 8-N_1*up* and hG-N_2*up,* were designed to hybridize

Con formato: Fuente: +Cuerpo (Calibri), 11 pto, Negrita, Inglés (Estados Unidos)

Con formato: Fuente: +Cuerpo (Calibri), Negrita, Inglés (Estados Unidos)

Con formato: Párrafo de lista, Sangría: Izquierda: 0 cm, Primera línea: 0 cm, Esquema numerado + Nivel: 2 + Estilo de numeración: 1, 2, 3, … + Iniciar en: 1 + Alineación: Izquierda + Alineación: 0,63 cm + Sangría: 1,4 cm

Con formato: Fuente: +Cuerpo (Calibri), 11 pto, Negrita, Inglés (Estados Unidos)

Con formato: Párrafo de lista, Esquema numerado + Nivel: 1 + Estilo de numeración: 1, 2, 3, … + Iniciar en: 1 + Alineación: Izquierda + Alineación: 0 cm + Sangría: 0,63 cm

Con formato: Fuente: 11 pto

Con formato: Fuente: +Cuerpo (Calibri), Negrita, Inglés (Estados Unidos)

Con formato: Párrafo de lista, Sangría: Izquierda: 0 cm, Primera línea: 0 cm, Espacio Después: 0 pto, Esquema numerado + Nivel: 2 + Estilo de numeración: 1, 2, 3, … + Iniciar en: 1 + Alineación: Izquierda + Alineación: 0,63 cm + Sangría: 1,4 cm, Punto de tabulación: 0,25 cm, Izquierda + No en 3,86 cm

Con formato: Espacio Antes: 0 pto

Código de campo cambiado

Código de campo cambiado

Código de campo cambiado

the *$N_y$downSH* oligonucleotides of the 20 and 40 nm AuNP size biohybrid multifunctional nanoparticles (AuNP20 and AuNP40), respectively. Additional hapten-oligonucleotide probes 13-*N_3up* and FQ-*N_4up*, for Boldenone (B) and Fluoroquinolones (FQ), respectively, were synthesized and used for control experiments (see table S1 for information on the oligonucleotide sequences)

Figure 1~~Figure 1~~ shows the biohybrid AuNP synthesized. For ST, AuNP20 were biofunctionalized with *N_3upSH* and *N_1downSH (*AuNP20-*N_3up/N_1down*)*, being this last oligonucleotide complementary to the 8-*N_1up* hapten-oligonucleotide probe, and *N_3upSH* complementary to the *N_3downNH$_2$* of the DNA microarray. In a similar manner, for THG, AuNP40 were functionalized with *N_4upSH* and *N_2downSH (*AuNP40-*N_4up/N_2down*),* being the last oligonucleotide sequence complementary to the hapten-oligonucleotide probe hG-*N_2up,* and *N_4upSH* complementary to *N_4downNH$_2$* oligonucleotide sequence of the DNA microarray (see Table 1~~Table 1~~ for a summary of the oligonucleotide sets and immunoreagents employed and table S1 for information on the oligonucleotide sequences). Additionally, so-called *negative* AuNP20 nanoparticles were prepared for control experiments containing only the *N_1downSH* strand, and therefore theoretically unable to bind to the DNA microarray.

3.2. Preparation of biofunctional nanostructured surfaces by DDI

AuNP20-*N_3up/N_1down* biohybrid nanoparticles were used on a first instance to demonstrate the viability of the immobilization approach by SEM. For this purpose, solutions of distinct concentrations of biofunctionalized nanoparticles were added to microarrays spotted with *N_3downNH$_2$* on a previously silanized glass slide. The SEM images in Figure 2~~Figure 2~~ A show that immobilization only occurred on those spots where the complementary strand (*N_3downNH$_2$*) had been previously immobilized, and no unspecific adsorption was observed outside the spots. Moreover, the particle density was clearly dependent on the concentration of the nanoparticles in the solution used while the distribution became more homogeneous as lower was the concentration (see Figure 2~~Figure 2~~ B). The biofunctionality of these nanostructured surfaces was assessed, by hybridizing these nanostructures with the ST hapten-oligonucleotide probe (8-*N_1up*) and running a non-competitive fluorescent immunoassay on *N_3downNH$_2$*-DNA microarrays. As can be observed in Figure 3~~Figure 3~~, fluorescence was only observed in those spots where the AuNP20-*N_3up/N_1down* nanoparticles and the positive control (N3: *13-N_3up* for B) had been added, while no signal was recorded on the microarrays incubated with *negative* AuNP20-DNA. These experiments confirmed the selective immobilization of the AuNP20-

Código de campo cambiado

Código de campo cambiado

Con formato: Fuente: 11 pto

Con formato: Párrafo de lista, Sangría: Izquierda: 0 cm, Primera línea: 0 cm, Espacio Después: 0 pto, Esquema numerado + Nivel: 2 + Estilo de numeración: 1, 2, 3, … + Iniciar en: 1 + Alineación: Izquierda + Alineación: 0,63 cm + Sangría: 1,4 cm, Punto de tabulación: 0,25 cm, Izquierda + No en 3,86 cm

Con formato: Fuente: +Cuerpo (Calibri), Negrita, Inglés (Estados Unidos)

Con formato: Espacio Antes: 0 pto

Código de campo cambiado

Código de campo cambiado

Código de campo cambiado

N_3up/N_1down through DDI on the glass microarray substrate. The positive control (N3) was used to check the biofunctionality of the *$N_3downNH_2$*-DNA microarray.

3.3. Multimodal biofunctional plasmonic nanostructures for AAS

The next goal was to achieve multimodal plasmonic nanostructured surfaces immobilizing selectively on different sites of a DNA microarray nanoparticles showing different RPs. For this purpose, solutions containing mixtures of AuNP20-*N_3up/N_1down* and AuNP40-*N_4up/N_2down,* were added to glass slides printed with 5x4 spot microarrays, but in which 5x2 had been spotted with *$N_3downNH_2$* (for ST) and 5x2 with *$N_4downNH_2$* (for THG). The SEM images could confirm that each multifunctional biohybrid nanoparticle was immobilized on their specific location of the microarray and that no cross-hybridization phenomena had taken place (see Figure 4~~Figure 4~~, B). As before, the biofunctionality of these substrates containing multifunctional gold nanoparticles of different sizes (AuNP20 and AuNP40) was assessed by non-competitive fluorescence immunoassay by adding the hapten-oligonucleotide probes, 8-*N_1up* (ST) and hG-*N2up* (THG) followed by the corresponding specific antisera (anti-ST, As147 and, anti-THG, As170) and anti-IgG-TRITC. In parallel, and as before, positive controls were run to check the correct immobilization of the capture oligonucleotides on the slide: control N3, for *$N_3downNH_2$* (followed by 13-*N_3up* and As138), and control N4, for *$N_4downNH_2$* (followed by FQ-*N_4up* and anti-FQ antiserum, As172). The results demonstrated that the nanostructured chip created by DDI, containing two types of nanoparticles, was biofunctional and that the response was selective for each target on the corresponding spots (see figure S2 in the SI document). Hence, *i)* the nanoparticles were appropriately located on the corresponding sites of the microarray, *ii)* the hapten-oligonucleotide probes had been appropriately hybridized on the right multifunctional AuNPs matching the DNA sequence and *iii)* the antibodies selectively bound to their targets in the corresponding locations of the microarray chip.

Subsequent competitive fluorescence immunoassays performed in the same type of microarrays demonstrated that the biofunctionality of the nanostructured surface allowed quantification of the selected target analytes (ST and THG, added as a 1:1 mixture at different concentrations) with a detectability in compliance with the minimum required performance limits (MRPLs) established by the World Anti-doping Agency (WADA), and comparable to that obtained using these immunoreagents in other formats (microplate-based ELISA (Salvador et al. 2007; Salvador et al. 2009; Tort et al. 2012b) and fluorescent microarray immunoassay (Tort et al. 2009)).

Figure 5~~Figure 5~~ shows the calibration curves obtained for ST and THG employing these multifunctional nanostructured surfaces and the tables in the right side show the analytical parameters. The microarray pictures in the left side show how the fluorescence response was observed, for each concentration, only on the corresponding spots of each microarray.

Con formato: Fuente: 11 pto

Con formato: Párrafo de lista, Sangría: Izquierda: 0 cm, Primera línea: 0 cm, Espacio Después: 0 pto, Esquema numerado + Nivel: 2 + Estilo de numeración: 1, 2, 3, … + Iniciar en: 1 + Alineación: Izquierda + Alineación: 0,63 cm + Sangría: 1,4 cm, Punto de tabulación: 0,25 cm, Izquierda + No en 3,86 cm

Con formato: Fuente: +Cuerpo (Calibri), Negrita, Inglés (Estados Unidos)

Código de campo cambiado

Código de campo cambiado

Código de campo cambiado

Código de campo cambiado

~~1.1.~~3.4. Multimodal multiplexed LSPR sensing

Next experiments were addressed to demonstrate the LSPR biosensing potential of these DDI-created multifunctional multimodal nanostructured surfaces. On a first instance the AuNP20-*N_3up/N_1down* and AuNP40-*N_4up/N_2down* biofunctionalized chips were characterized for their LSPR spectra, recording the scattered light of the different sites of the microarray chip. Since the difference in the LSPR peak of spherical nanoparticles is very similar, both sites of the chip showed similar LSPR spectra with a peak between 570 and 580 nm (see Figure 4~~Figure 4~~ C, colored dotted lines), red-shifted in respect to the usual RP of bared nanoparticles (520-530 nm, data not shown) due to the change in the refractive index of the nanoparticle surrounding media produced by the charge of the oligonucleotides(Schneider et al. 2013). Hybridization with the hapten-oligonucleotide probes produced an additional shift to higher wavelengths (see Figure 4~~Figure 4~~ C, black dotted lines). The shift was greater for the AuNP40-*N_4up/N_2down* biofunctionalized chips probably due to the higher number of hapten-oligonucleotide probes captured by these particles. For biosensing purposes these RP spectra were the offset of the measurements. It should be mentioned that one of the main problems encountered on these experiments was related to the presence of salt residues remaining from the buffer solutions on the surfaces, which strongly scattered the light masking the one scattered by the nanoparticles, and that the problem was solved washing the slides with care with 0.3 M ammonium acetate buffer, pH 7.0 (Demers et al. 2002) before the LSPR measurements as it is described in the experimental section.

These multiplexed multimodal chips were exposed then to blank samples (no analytes) and to samples containing mixtures of ST and THG (1000 nM) together with the antibodies (ST, As147 and THG, As170). After a short incubation time, the chips were washed and the LSPR spectra were recorded. In this case a significant blue shift (towards lower wavelengths, about 23 and 35 nm for THG and ST, respectively) of the LSPR spectra was observed when the samples did not contain analyte due to the binding of the specific antibodies to the hapten-oligonucleotide probes immobilized on the corresponding sites in the nanostructured chip (see Figure 4~~Figure 4~~ C, bold colored lines). In contrast, no significant shift was observed when the chips were exposed to ST and/or THG solutions at 1000 nM concentration, indicating that a complete inhibition of the antibody binding to the chip had taken place due to the presence of high concentrations of the analytes (see Figure 4~~Figure 4~~ C, light colored lines over overlaying the black dotted line). Since these results already pointed to the high detectability that could be accomplished with these chips, a preliminary LSPR calibration experiment was performed in buffer by measuring a set of ST calibrators on AuNP20-*N_3up/N_1down* (*8-N1up*) biofunctionalized nanostructured chips.

Código de campo cambiado

Código de campo cambiado

Código de campo cambiado

Código de campo cambiado

Código de campo cambiado

Código de campo cambiado

A dose-dependent relationship was obtained when plotting the shift of the RP of the chips that had been exposed to different concentrations of ST (see Figure 6~~Figure 6~~). The results indicate that, under non-optimized conditions, ST concentration values down to 2 nM could still be distinguished from zero in these experiments (statistically significant at $P < 0.05$ with a confidence level of 95%).

Therefore, the results shown in this paper demonstrate that DDI may be used to manufacture multiplexed multimodal plasmonic nanostructures with a high potential for highly sensitive LSPR biosensing applications. At this point it should be noticed that with the equipment used in this work, the intensity of the signal recorded on the 20 nm AuNP spots was very low. More intense and narrower peaks, and consequently much better and reproducible results, could be obtained using nanoparticles of a greater size (about 80 nm), since contribution of scattering to the extinction rapidly increase with the size (Jain et al. 2006), or with different shapes (i.e. nanorods). Another aspect that would need to be optimized is the distribution of the nanoparticles in the surface chip during the different fabrication batches, which lead to certain variability regarding LSPR response. Moreover, in the actual sensor configuration shown in this paper, a final washing step with distilled water would remove not only the oligonucleotide probes, but also the nanoparticles from the surface. Thus, there will be necessary to explore alternative strategies to provide stronger stability to the first hybridization step (N_x*down*-microarray- N_x*up*/N_y*down-AuNP*) such as for example using of PNA/DNA duplexes(Nielsen and Egholm 1999) or modified bases with possibilities for cross-linking(Stephenson et al. 2011; Wang et al. 2016; Zhang and Paukstelis 2016) etc.). On a recent paper, Tomàs Gamasa et al.(Tomas-Gamasa et al. 2015) have reported formation of selective, reversible and highly thermostable DNA interstrand cross-links based on the reversible imine chemistry concept. This approach would allow dehybridizing the hapten-oligonucleotide conjugates without removing the gold nanoparticles from the surface, to use the multimodal nanostructured chip on further analysis with the same or a different set of N_y*up* biomolecular probes, being also possible to recover the DNA microarray when required to immobilize a distinct set of multifunctional nanoparticles.

CONCLUSIONS

Multimodal plasmonic nanostructured surfaces have been created through DNA-directed immobilization of multifunctional biohybrid gold nanoparticles through simple DNA hybridization. These surfaces have been characterized by SEM, fluorescence and LSPR. The fact that AuNP with different optical properties and functionalities could easily be selectively

Código de campo cambiado

Código de campo cambiado

Con formato: Fuente: Cursiva

Con formato: Fuente: Cursiva, Subíndice

Código de campo cambiado

Código de campo cambiado

Código de campo cambiado

immobilized on different sites of a surface opens the possibility to develop sophisticated plasmonic nanostructures combining nanoparticles of different sizes, shapes or composition.

The results shown in this paper are a demonstration of the potential of DDI to develop a label-free multiplexed multimodal LSPR immunosensor platforms. This approach takes advantage of the well-established DNA microarray manufacturing procedures by easily converting them on LSPR chips, by just hybridizing the surface with the corresponding set of multifunctional biohybrid nanoparticles. The approach here presented uses oligonucleotide encoded AuNPs for directing immobilization (series N_x*upSH*) on a DNA microarray but also for further specific biofunctionalization (series N_y*downSH*) with oligonucleotide codified bioreceptors whose DNA sequence is complementary (series N_y*up*). Therefore, it can be considered as a universal approach for manufacturing multiplexed LSPR chips with different sets of bioreceptors depending on the application. In this work, as proof-of-concept, we have addressed the detection of small organic molecules such as the AAS, and for this purpose, we have hybridized the immobilized nanoparticles with hapten-N_y*up* probes. Preliminary results obtained indicate that detectability achieved can be in the same order as other immunochemical detection systems using labels or amplification approaches. Although in this case identification of the target analyte has only been possible because of the use of site-encoded chips, due to the close RP of the spherical nanoparticles used, the approach could also be used for immobilizing sets of nanoparticles differing on shape or material, and therefore showing distinct plasmonic properties, which would allow developing chips with a dual identification mode based on the site codification and on the RP. Future challenges of this research would be focused on the development of more robust LSPR biosensors and also on demonstrating the possibility to regenerate these biofunctional nanostructured surfaces.

ACKNOWLEDGMENTS

The authors would like to acknowledge Prof. R. Eritja (IQAC-CSIC, Barcelona, Spain) for his scientific advice and supplying some the oligonucleotides employed in this work, to Prof. Gonçal Badenes and Dr. Romain Quidant (ICFO, Castelldefells, Barcelona, Spain) for the scientific discussions on LSPR and to Prof. L. Lechuga (ICN2, Bellaterra, Barcelona, Spain) for giving us the opportunity to use a dark-field microscope from her laboratory in the initial steps of this research. This work has been supported by the MINECO (Spanish Ministry of Economy and Competitiveness) in the frame OligoCODEs (MAT2012-38573-C02-01) and Immuno-QS (SAF2015-67476-R) projects. The Nb4D group (formerly Applied Molecular Receptors group, AMRg) is a consolidated research group of the Generalitat de Catalunya and has support from the

Departament d'Universitats, Recerca i Societat de la Informació de la Generalitat de Catalunya (expedient : 2014 SGR 1484). CIBER-BBN is an initiative funded by the Spanish National Plan for Scientific and Technical Research and Innovation 2013-2016, Iniciativa Ingenio 2010, Consolider Program, CIBER Actions are financed by the Instituto de Salud Carlos III with assistance from the European Regional Development Fund. The ICTS "NANOBIOSIS", and particularly the Custom Antibody Service (CAbS, IQAC-CSIC, CIBER-BBN), is acknowledged for the assistance and support related to the immunoreagents used in this work.

FIGURE LEGENDS

Figure 1: Multifunctional biohybrid nanoparticles. ***Left****:* General scheme showing the distinct oligonucleotide probes used. Each nanoparticle is codified with two different oligonucleotide strands which are shown as wave lines of two distinct colors for selective functionalization with the corresponding hapten and immobilization on the DNA microarray. Each oligonucleotide sequence is identified as Nx plus the words *down* or *up*. The oligonucleotide series *down* are designed to hybridize with the corresponding hapten-oligonucleotide conjugate bearing the complementary oligonucleotide sequence. The oligonucleotide series *up* is designed to hybridize with the complementary oligonucleotide sequence immobilized on the DNA microarray chip for site codification of the AuNPs ***Right****:* of AuNP-DNA probes prepared and employed in this work; ***Right-Top****:* AuNP20-N_3up/N_1down called *positive,* designed to detect ST, are 20 nm size gold nanoparticles biofunctionalized with N_3upSH, complementary to N_3dowNH_2 oligonucleotides immobilized on the chip, and N_1down, complementary to the hapten oligonucleotide probe 8-N_1up; ***Right-Middle:*** AuNP20-N_1down called *negative,* lacking the oligonucleotide chain that hybridizes with the DNA-chip; ***Right-Bottom:*** AuNP40-N_4up/N_2down also called *positive,* designed to detect THG, are 40 nm AuNP biofunctionalized with N_4upSH, *for hybridization with the* $N_4downNH_2$ oligonucleotides of the DNA chip, *and* $N_2downSH$, for hybridization with the hapten oligonucleotide probe hG-N_2up. See Table 1~~Table 1~~ for additional information of the oligonucleotide sets used and Table S1 for the oligonucleotide sequences.

Figure 2~~Figure 2~~: Surface electron microscopy (SEM) images of nanostructured surfaces prepared by the DNA-directed immobilization of the AuNP20-N_3up/N_1down nanoprobes. **A**: Microscope images of one microarray chip, printed with a 5x4 spot matrix of N_3dowNH_2 oligonucleotides. The enlarged microscope image in the right, shows the edge of one of the spots, where it can be noticed that there is no unspecific absorption outside the spots, and that the gold nanoparticles have been immobilized selectively inside the spots where its complementary oligonucleotide strand was previously immobilized. **B:** Spot SEM images of AuNP microarrays prepared using different concentrations of *AuNP20-N3up/N1down* nanoprobes. It can be shown how the isolated AuNP density can be controlled.

Figure 3~~Figure 3~~: Selectivity of DNA-directed immobilization of AuNP demonstrated by fluorescence immunoassay. **A:** Graph showing the relative florescence units (RFUs) recorded after performing the immunoassay on DNA microarrays previously exposed to positive (*AuNP20-N3up/*N_1down) and negative AuNP20 (*AuNP20-*N_1down). 13-N_3up was used as positive control to ensure performance of DNA-microarray manufacture and of the fluorescence immunoassay.

Con formato: Color de fuente: Automático

Con formato: Color de fuente: Automático

Código de campo cambiado

Código de campo cambiado

Con formato: Fuente: Negrita

Código de campo cambiado

Con formato: Fuente: Negrita

As expected the positive AuNP20 and control N3 provided significant fluorescence, while the negative AuNP20 did not. **B:** Fluorescent images of the 5x2 microarray matrices (*N_3downNH_2*) corresponding to the above mentioned experiments. **C:** Schemes of the experimental conditions showing the on each case the oligonucleotide codified AuNPs and the antibodies used. The oligonucleotide sequences are indicated on top of each scheme. For the antibodies As147, against ST, is shown in blue and As170, for THG, is shown in green. The red antibody is antiIgG-TRITC. Results shown are the average of the signal recorded in 4 different microarrays.

Figure 4~~Figure 4~~: Multiplexed LSPR microarray chip for simultaneous determination of stanozolol (ST) and tetrahydrogestrinone (THG). **A**: Scheme of the multiplexed LSPR immunosensor chip showing how specific antibodies against ST and THG bind to their corresponding hapten previously immobilized on the surface of the nanostructured chip surface or to the free analyte. As147, against ST, is shown in blue and As170, for THG, is shown in green **B:** SEM images of the multifunctional nanostructured surface prepared through DNA-directed immobilization of a cocktail of distinct AuNP-DNA nanoprobes (*AuNP20-N3up/N1down* and AuNP40-*N_4up/N_2down*) on different spots of a 5x4 microarray chip. The SEM images demonstrate the selectivity of the approach, showing how the AuNP20 (top, for ST detection) and AuNP40 (bottom, for THG detection) have been addressed to the corresponding spots where their corresponding complementary DNA chains have been previously immobilized. **C:** Graphs of the scattered light recorded on the different sites of the chip where the two types of multifunctional nanoparticles have been immobilized. The colored dotted lines shows the LSPR spectra of the multifunctional LSPR chip resulting from immobilizing the two AuNP-DNA nanoprobes and the black dotted lines are the LSPR spectra after hybridization with the corresponding hapten-oligonucleotide probes. The colored bold lines show the LSPR spectra recorded after exposing the chip to a solution containing a cocktail of specific antibodies in the absence of the target analytes (maximum antibody binding). The colored light lines are the LSPR spectra recorded under the same conditions but in this case the solution contained THG and ST at 1000 nM (complete inhibition of the antibody binding to the LSPR chip).

Figure 5~~Figure 5~~: Results from the evaluation of the biofunctionality of the multifunctional nanostructured chips by fluorescence immunoassay. After hybridization with a cocktail of the ST and THG hapten-oligonucleotide probes (8-*N_1up* and hG-*N_2up*, respectively) the chips were used

Con formato: Color de fuente: Automático

Código de campo cambiado

Con formato: Fuente: Negrita

Con formato: Color de fuente: Automático

Con formato: Normal, Justificado, Espacio Antes: Automático, Después: Automático, Interlineado: 1,5 líneas

Código de campo cambiado

Con formato: Color de fuente: Automático

to run calibration curves using fluorescent labelled secondary antibodies. In these experiments, different microarray slides were used to run the ST or the THG fluoroimmunoassays. ***A:*** Pictures of the microarray slides used on the calibration experiments and showing how the fluorescence only appears on the corresponding spots of the slide for each analyte and that the intensity is dependent of the analyte concentration. **B:** Calibration graphs for ST (top) and THG (bottom). Negligible background signal was recorded on the spots where the contrary hapten-oligonucleotide had been hybridized. **C:** Tables showing the analytical features of the microarray ST (top) and THG (bottom) fluorescence immunoassays. Each data point corresponds to the average of 30 spots. The results show that the LSPR multiplexed chip is biofunctional and shows excellent analytical features.

Figure 6~~Figure 6~~: Performance of the ST LSPR immunosensor. The bar graph shows the LSPR response of distinct chips to the presence of distinct concentrations of ST. The values shown are the average and standard deviation of measurements made in 5 different chips with a 5x4 spot microarray matrix of *AuNP20-N3up/N1down (8-N1up).* The asterisk indicates a statistical significance of $P < 0.05$ (confidence level 95%).

Código de campo cambiado

Con formato: Fuente: Negrita

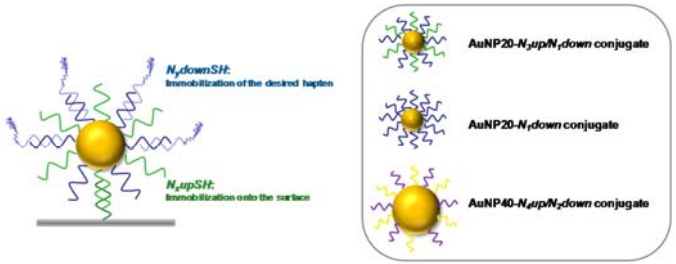

Figure 1

Código de campo cambiado

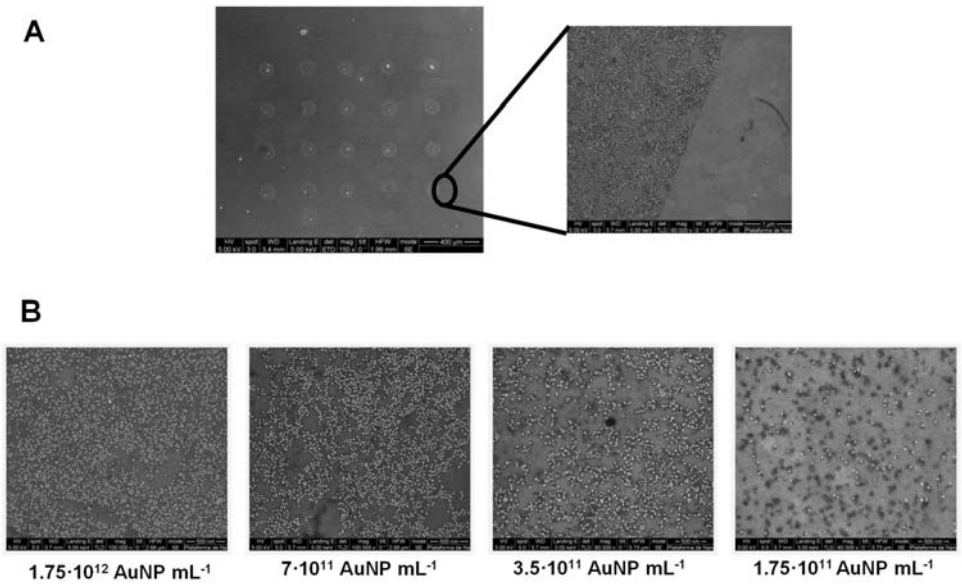

Figure 2

Código de campo cambiado

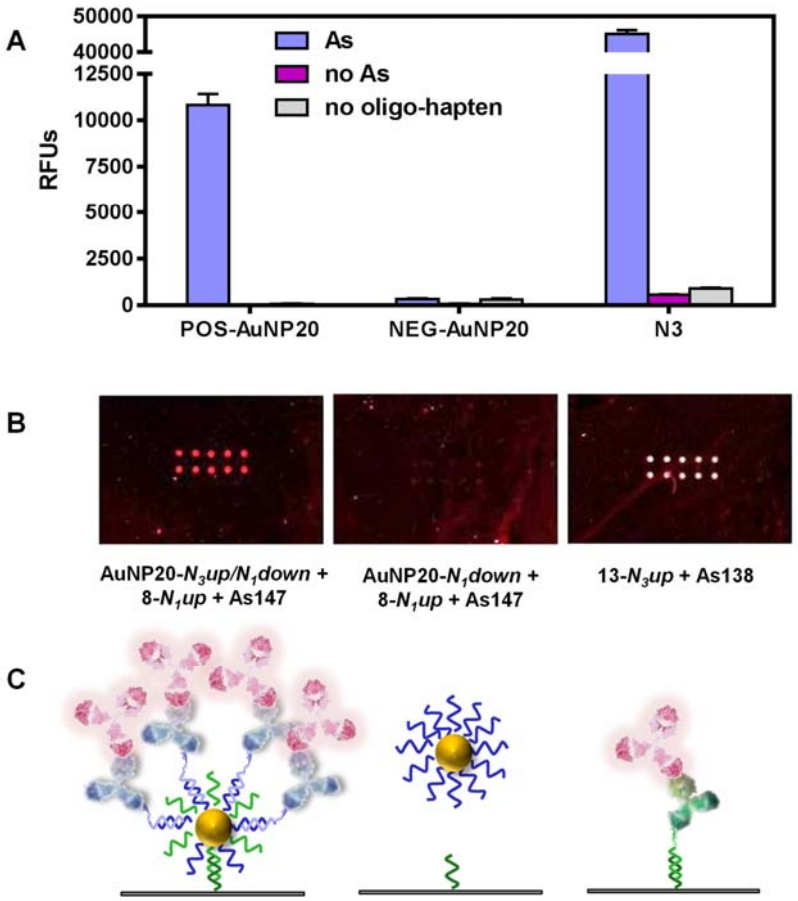

Figure 3

Código de campo cambiado

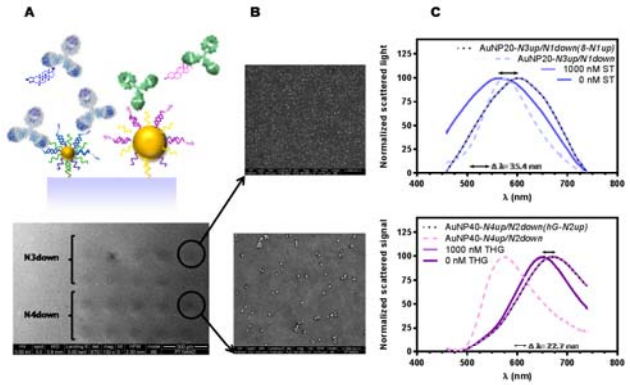

Figure 4

Código de campo cambiado

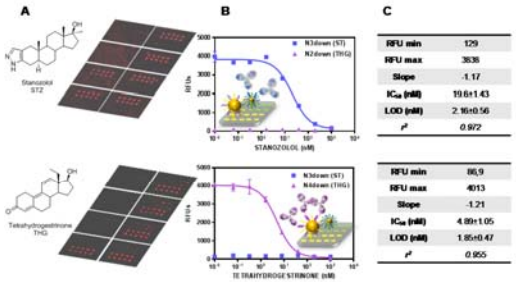

C	
RFU min	129
RFU max	3836
Slope	-1.17
IC_{50} (nM)	19.6±1.43
LOD (nM)	2.16±0.56
r^2	0.972

RFU min	86,9
RFU max	4013
Slope	-1.21
IC_{50} (nM)	4.89±1.05
LOD (nM)	1.85±0.47
r^2	0.955

Figure 5

Código de campo cambiado

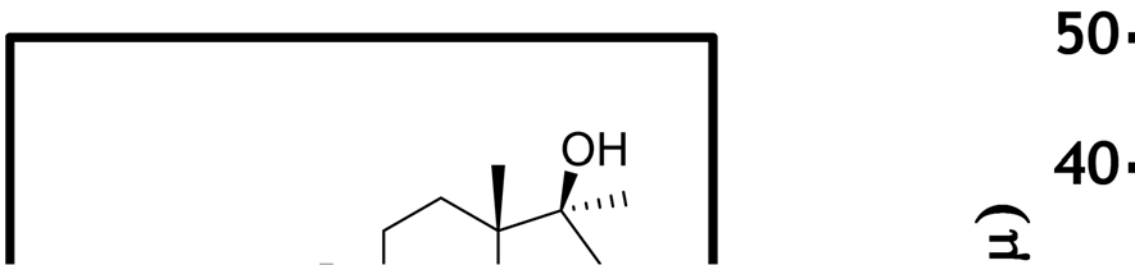

Figure 6

Código de campo cambiado

Table 1: List of all the reagents employed in the multiplexed studies.

TARGET	DNA Microarray (*down series*)	AuNP-DNA (*up series*)	AuNP-DNA (*down series*)	Hapten-DNA (*up series*)	As
Stanozolol (ST)	*N_3downNH$_2$*	*N_3upSH*	*N_1downSH*	8-*N_1up*	As14
Tetrahydrogestrinone (THG)	*N_4downNH$_2$*	*N_4upSH*	*N_2downSH*	hG-*N_2up*	As17
Control N3	*N_3downNH$_2$*			13-*N_3up*	As13
Control N4	*N_4downNH$_2$*			FQ-*N_4up*	As17

REFERENCES

Anker, J.N., Hall, W.P., Lyandres, O., Shah, N.C., Zhao, J., Van Duyne, R.P., 2008. Biosensing with plasmonic nanosensors. Nat Mater 7(6), 442-453.

Bhushan, B., Matsui, S., 2010. Three-Dimensional Nanostructure Fabrication by Focused Ion Beam Chemical Vapor Deposition. Springer Handbook of Nanotechnology, pp. 211-229. Springer Berlin Heidelberg.

Bohren, C.F.H., D. R. , 1983. Absorption and scattering of light by small particles. Wiley-Interscience.

Brown, K.R., Walter, D.G., Natan, M.J., 1999. Seeding of Colloidal Au Nanoparticle Solutions. 2. Improved Control of Particle Size and Shape. Chemistry of Materials 12(2), 306-313.

Calvo, D., Salvador, J.P., Tort, N., Centi, F., Marco, M.P., Marco, S., 2009. Multidetection of anabolic androgenic steroids using immunoarrays and pattern recognition techniques. AIP Conference Proceedings, pp. 547-550.

Demers, L.M., Ginger, D.S., Park, S.J., Li, Z., Chung, S.W., Mirkin, C.A., 2002. Direct Patterning of Modified Oligonucleotides on Metals and Insulators by Dip-Pen Nanolithography. Science 296(5574), 1836-1838.

Enustun, B.V.a.T., J., 1963. COAGULATION OF COLLOIDAL GOLD. Journal of the American Chemical Society 85(21), 3317-&.

Estevez, M.C., Marinus A. Otte, Sepulveda, B., Lechuga, L.M., 2014. Trends and challenges of refractometric nanoplasmonic biosensors: A review. Analytica Chimica Acta 806, 55-73.

Frens, G., 1973. Controlled Nucleation for the Regulation of the Particle Size in Monodisperse Gold Suspensions. Nature Physical Science 241(1), 20-22.

Fujiwara, K., Watarai, H., Itoh, H., Nakahama, E., Ogawa, N., 2006. Measurement of antibody binding to protein immobilized on gold nanoparticles by localized surface plasmon spectroscopy. Analytical and Bioanalytical Chemistry 386(3), 639-644.

Grabar, K.C., Freeman, R.G., Hommer, M.B., Natan, M.J., 1995. Preparation and Characterization of Au Colloid Monolayers. Analytical Chemistry 67(4), 735-743.

Graells, S.A., R.; Badenes, G. and Quidant, R. , 2007. Growth of plasmonic gold nanostructures by electron beam induced deposition. Appl. Phys. Lett. 91( ), 121112-121111/121113.

Guillot, N., de la Chapelle, M.L., 2012. Lithographied nanostructures as nanosensors. Journal of Nanophotonics 6.

Haiss, W., Thanh, N.T.K., Aveyard, J., Fernig, D.G., 2007. Determination of Size and Concentration of Gold Nanoparticles from UVâˆ'Vis Spectra. Analytical Chemistry 79(11), 4215-4221.

Hill, H.D., Mirkin, C.A., 2006. The bio-barcode assay for the detection of protein and nucleic acid targets using DTT-induced ligand exchange. Nat. Protocols 1(1), 324-336.

Hill, R.T., 2015. Plasmonic biosensors. Wiley Interdisciplinary Reviews-Nanomedicine and Nanobiotechnology 7(2), 152-168.

Hu, M., Chen, J., Li, Z.-Y., Au, L., Hartland, G.V., Li, X., Marquez, M., Xia, Y., 2006. Gold nanostructures: engineering their plasmonic properties for biomedical applications. Chemical Society Reviews 35(11), 1084-1094.

Jain, P.K., Lee, K.S., El-Sayed, I.H., El-Sayed, M.A., 2006. Calculated Absorption and Scattering Properties of Gold Nanoparticles of Different Size, Shape, and Composition:â€‰ Applications in Biological Imaging and Biomedicine. The Journal of Physical Chemistry B 110(14), 7238-7248.

Klinkova, A., Choueiri, R.M., Kumacheva, E., 2014. Self-assembled plasmonic nanostructures. Chemical Society Reviews 43(11), 3976-3991.

Kreuzer, M., Quidant, R., Salvador, J.P., Marco, M.P., Badenes, G., 2008. Colloidal-based localized surface plasmon resonance (LSPR) biosensor for the quantitative determination of stanozolol. Analytical and Bioanalytical Chemistry 391(5), 1813-1820.

Código de campo cambiado

Kreuzer, M.P., Quidant, R., Badenes, G., Marco, M.P., 2006. Quantitative detection of doping substances by a localised surface plasmon sensor. Biosensors and Bioelectronics 21(7), 1345-1349.
Li, W., Zhang, L., Zhou, J., Wu, H., 2015. Well-designed metal nanostructured arrays for label-free plasmonic biosensing. Journal of Materials Chemistry C 3(25), 6479-6492.
Li, X., Jiang, L., Zhan, Q., Qian, J., He, S., 2009. Localized surface plasmon resonance (LSPR) of polyelectrolyte-functionalized gold-nanoparticles for bio-sensing. Colloids and Surfaces A: Physicochemical and Engineering Aspects 332(2-3), 172-179.
Liz-Marzán, L.M., 2005. Tailoring Surface Plasmons through the Morphology and Assembly of Metal Nanoparticles. Langmuir 22(1), 32-41.
Loweth, C.J., Caldwell, W.B., Peng, X., Alivisatos, A.P., Schultz, P.G., 1999. DNA-Based Assembly of Gold Nanocrystals. Angewandte Chemie International Edition 38(12), 1808-1812.
Lv, J., Leong, E.S.P., Jiang, X., Kou, S., Dai, H., Lin, J., Liu, Y.J., Si, G., 2015. Plasmon-Enhanced Sensing: Current Status and Prospects. Journal of Nanomaterials.
Mannelli, I., Marco, M.P., 2010. Recent advances in analytical and bioanalysis applications of noble metal nanorods. Analytical and Bioanalytical Chemistry 398(6), 2451-2469.
Mayer, K.M., Hafner, J.H., Localized Surface Plasmon Resonance Sensors. Chemical Reviews 111(6), 3828-3857.
Meyer, R., Giselbrecht, S., Rapp, B.E., Hirtz, M., Niemeyer, C.M., 2014. Advances in DNA-directed immobilization. Current Opinion in Chemical Biology 18, 8-15.
Nielsen, P.E., Egholm, M., 1999. An Introduction to Peptide Nucleic Acid. Current Issues Molec. Biol. 1(2), 89-104.
Peschel, S., Ceyhan, B., Niemeyer, C.M., Gao, S., Chi, L., Simon, U., 2002. Immobilization of gold nanoparticles on solid supports utilizing DNA hybridization. Materials Science and Engineering: C 19(1-2), 47-50.
Petryayeva, E., Krull, U.J., 2011. Localized surface plasmon resonance: Nanostructures, bioassays and biosensing-A review. Analytica Chimica Acta 706(1), 8-24.
Pinacho, D.G., Sánchez-Baeza, F., Marco, M.P., 2012. Molecular Modeling Assisted Hapten Design To Produce Broad Selectivity Antibodies for Fluoroquinolone Antibiotics. Analytical Chemistry 84(10), 4527-4534.
Reichert, J.r., CsÃ¡ki, A., KÃ¶hler, J.M., Fritzsche, W., 2000. Chip-Based Optical Detection of DNA Hybridization by Means of Nanobead Labeling. Analytical Chemistry 72(24), 6025-6029.
Reinhard, B.r.M., Siu, M., Agarwal, H., Alivisatos, A.P., Liphardt, J., 2005. Calibration of Dynamic Molecular Rulers Based on Plasmon Coupling between Gold Nanoparticles. Nano Letters 5(11), 2246-2252.
Salvador, J.-P., Sanchez-Baeza, F., Marco, M.-P., 2007. Preparation of Antibodies for the Designer Steroid Tetrahydrogestrinone and Development of an Enzyme-Linked Immunosorbent Assay for Human Urine Analysis. Anal. Chem. 79(10), 3734-3740.
Salvador, J.P., Sánchez-Baeza, F., Marco, M.P., 2008. Simultaneous immunochemical detection of stanozolol and the main human metabolite, 3'-hydroxy-stanozolol, in urine and serum samples. Analytical Biochemistry 376(2), 221-228.
Salvador, J.P., Sánchez-Baeza, F., Marco, M.P., 2009. A high-throughput screening (HTS) immunochemical method for the analysis of stanozolol metabolites in cattle urine samples. Journal of Chromatography B 878(2), 243-252.
Schneider, T., Jahr, N., Jatschka, J., Csaki, A., Stranik, O., Fritzsche, W., 2013. Localized surface plasmon resonance (LSPR) study of DNA hybridization at single nanoparticle transducers. Journal of Nanoparticle Research 15(4), 1-10.
Seymour, E., Daaboul, G.G., Zhang, X., Scherr, S.M., Unlu, N.L., Connor, J.H., Uenlue, M.S., 2015. DNA-Directed Antibody Immobilization for Enhanced Detection of Single Viral Pathogens. Analytical Chemistry 87(20), 10505-10512.
Sonnichsen, C., Reinhard, B.M., Liphardt, J., Alivisatos, A.P., 2005. A molecular ruler based on plasmon coupling of single gold and silver nanoparticles. Nat Biotech 23(6), 741-745.

Sriram, M., Zong, K., Vivekchand, S.R.C., Gooding, J.J., 2015. Single Nanoparticle Plasmonic Sensors. Sensors 15(10), 25774-25792.
Stephenson, A.W.I., Partridge, A.C., Filichev, V.V., 2011. Synthesis of beta-Pyrrolic-Modified Porphyrins and Their Incorporation into DNA. Chemistry-a European Journal 17(22), 6227-6238.
Tan, L.H., Xing, H., Lu, Y., 2014. DNA as a Powerful Tool for Morphology Control, Spatial Positioning, and Dynamic Assembly of Nanoparticles. Accounts of Chemical Research 47(6), 1881-1890.
Taton, T.A., 2001. Preparation of Gold Nanoparticle–DNA Conjugates. John Wiley & Sons, Inc.
Tomas-Gamasa, M., Serdjukow, S., Su, M., Mueller, M., Carell, T., 2015. "Post-It" Type Connected DNA Created with a Reversible Covalent Cross-Link. Angewandte Chemie-International Edition 54(3), 796-800.
Tort, N., Salvador, J.P., Aviñó, A., Eritja, R., Comelles, J., Martínez, E., Samitier, J., Marco, M.P., 2012a. Synthesis of Steroid–Oligonucleotide Conjugates for a DNA Site-Encoded SPR Immunosensor. Bioconjugate Chemistry 23(11), 2183-2191.
Tort, N., Salvador, J.P., Marco, M.P., 2012b. Multiplexed immunoassay to detect anabolic androgenic steroids in human serum. Analytical and Bioanalytical Chemistry 403(5), 1361-1371.
Tort, N., Salvador, J.P., Marco, M.P., Eritja, R., Poch, M., Martínez, E., Samitier, J., 2009. Fluorescence site-encoded DNA addressable hapten microarray for anabolic androgenic steroids. TrAC Trends in Analytical Chemistry 28(6), 718-728.
Turkevich, J.S., P.C.; Hillier, J.; , 1951. Discussions of the Faraday Society 11, 55-75.
Wang, Y., Liu, S., Lin, Z., Fan, Y., Wang, Y., Peng, X., 2016. Photochemical Generation of Benzyl Cations That Selectively Cross-Link Guanine and Cytosine in DNA. Organic Letters 18(11), 2544-2547.
Wang, Z., Ma, L., 2009. Gold nanoparticle probes. Coordination Chemistry Reviews 253(11-12), 1607-1618.
Willets, K.A., Van Duyne, R.P., 2007. Localized Surface Plasmon Resonance Spectroscopy and Sensing. Annual Review of Physical Chemistry 58(1), 267-297.
Wolfgang, F., Taton, T.A., 2003. Metal nanoparticles as labels for heterogeneous, chip-based DNA detection. Nanotechnology 14(12), R63.
Yamamichi, J., Iida, M., Ojima, T., Handa, Y., Yamada, T., Kuroda, R., Imamura, T., Yano, T., 2009. The mesoscopic effect on label-free biosensors based on localized surface plasmon resonance of immobilized colloidal gold. Sensors and Actuators B: Chemical 143(1), 349-356.
Yu, C., Irudayaraj, J., 2007. Multiplex Biosensor Using Gold Nanorods. Anal. Chem. 79(2), 572-579.
Zhang, D., Paukstelis, P.J., 2016. Enhancing DNA Crystal Durability through Chemical Crosslinking. Chembiochem 17(12), 1163-1170.
Zhao, J., Zhang, X., Yonzon, C.R., Haes, A.J., Van Duyne, R.P., 2006. Localized surface plasmon resonance biosensors. Nanomedicine 1(2), 219-228.
Zhou, B., Xiao, X., Liu, T., Gao, Y., Huang, Y., Wen, W., 2016. Real-time concentration monitoring in microfluidic system via plasmonic nanocrescent arrays. Biosensors & Bioelectronics 77, 385-392.